A SECOND LOOK AT THE LEAST-SQUARES ALGORITHM FOR RECOVERING INFORMATION FROM OPTICAL FLOW

S J Maybank
Marconi Command and Control Systems Ltd
Technology Group
Chobham Road
Frimley
Camberley
Surrey GU16 5PE

ABSTRACT

An algorithm for recovering some of the parameters of the motion of a rigid environment from the associated optical flow field is analysed in the special case of an optical flow field arising from an irregular moving rigid surface. The results of the analysis are checked using computer-generated optical flow fields.

I BACKGROUND AND NOTATION

The changes in an image arising from the motion of the environment have been intensively studied over the past few years [2,3,4,5,7]. These changes, termed optical flow, depend on both the motion and the shape of the environment. The central problem in the study of optical flow is to find the best way of recovering information about the motion and shape of the environment from the associated optical flow field.

It is shown in [3,4] that some parameters of the motion can be recovered with greater accuracy than the remaining parameters, provided the optical flow field arises from an irregular moving rigid surface. This result is obtained by analysing a particular algorithm for recovering information from an optical flow field, but it is conjectured that a similar result holds for a wide class of such algorithms. The term 'irregular' refers to the three-dimensional shape of the surface, not to its texture. A surface is classed as irregular if the set of inverse distances to points on the surface does not possess a good linear approximation.

The algorithm in question is based on a least-squares error function $\varepsilon(\underline{v})$, which is defined below. A preliminary analysis of $\varepsilon(\underline{v})$ is given in [3]. The analysis of $\varepsilon(\underline{v})$ is continued in this paper because of its great importance. To the author's knowledge, no comparable analysis of any other algorithm for recovering information from an optical flow field associated with a general rigid motion is available, in spite of the practical importance of the subject, and in spite of the great number of algorithms that have been published.

In the case of an optical flow field arising from an irregular moving rigid surface, there is a simple approximation to $\varepsilon(\underline{v})$ which can be used to predict the performance of the least-squares algorithm in situations of practical interest [3,4]. In this paper an upper bound is obtained for the difference between $\varepsilon(\underline{v})$ and this approximation. The analysis of $\varepsilon(\underline{v})$ in the case of optical flow fields arising from smooth surfaces appears to be difficult, and it is not attempted.

Experimental results show that the approximation to $\varepsilon(\underline{v})$ is astonishingly accurate. The analysis given below provides only a partial explanation for this accuracy, since the difference between $\varepsilon(\underline{v})$ and its approximation is often several times larger than the bounds on this difference obtained theoretically. Further results concerning this approximation may be found in [4].

The optical flow fields under consideration are those associated with the image of a rigid environment formed by polar projection onto the unit sphere centred at the projection point [2,4,5,7]. The translational and angular velocities of the environment relative to the camera are denoted by $\hat{\underline{v}}$, $\hat{\underline{\Omega}}$ respectively. The angular velocity, $\hat{\underline{\Omega}}$, is taken about an axis through the projection point. Once the axis for the angular velocity is fixed, $\hat{\underline{v}}$ and $\hat{\underline{\Omega}}$ are uniquely determined by the motion of the environment relative to the camera [6]. It is assumed that $\hat{\underline{v}} \neq 0$.

It is assumed that the velocities across the projection sphere, $\dot{\underline{Q}}_i$, of features in the image are available at points $\underline{Q}_i$ on the projection sphere $(1 \leq i \leq n)$, at one particular instant of time. It is shown in [2,4] that if the environment is rigid then the $\dot{\underline{Q}}_i$ are given in terms of the motion and shape of the environment as follows.

$$\dot{\underline{Q}}_i = [\hat{\underline{v}} - (\hat{\underline{v}} \cdot \underline{Q}_i)\underline{Q}_i]K_i + \hat{\underline{\Omega}} \times \underline{Q}_i \qquad (1)$$

where K_i^{-1} is the distance to the rigid body surface in the direction $\underline{Q}_i$ and $\times$ denotes the cross product of vectors [6]. The vector $\underline{Q}_i$ is often referred to as the base point of $\dot{\underline{Q}}_i$. The vector $\underline{Q}$ (without a subscript) is, by definition, equal to $(0, 0, 1)^T$.

Throughout this paper the index i ranges over the set $\{1, \ldots, n\}$. The range $(1 \leq i \leq n)$ will not be stated explicitly.

It is well known that the magnitude of $\hat{\underline{v}}$ and the absolute values of the inverse distances K_i cannot be recovered from the optical flow field alone [2,4,5]. If $\{\hat{\underline{v}}, K_i, \hat{\underline{\Omega}}\}$ is a set of solutions to (1), then $\{\hat{\underline{v}}/c, cK_i, \hat{\underline{\Omega}}\}$ is also a set of solutions to (1) for any value of the constant c. For this reason it is assumed, without loss of generality, that $\|\hat{\underline{v}}\| = 1$, where $\|\cdot\|$ denotes the Euclidean vector norm.

The vectors $\underline{v}$, $\underline{\Omega}$ are used to denote trial values of $\hat{\underline{v}}$, $\hat{\underline{\Omega}}$, respectively. The vector $\underline{v}$ may be any unit vector and $\underline{\Omega}$ may be any vector in $\mathbb{R}^3$. In particular, it is not assumed that $\underline{v}$, $\underline{\Omega}$ are compatible with the optical flow field. The vector $\underline{v} \times \hat{\underline{v}}$ is denoted by $\underline{a}$. The component of $\underline{a}$ used most frequently in this paper is

$$a_3 = v_1\hat{v}_2 - v_2\hat{v}_1.$$

AVC 1987 doi:10.5244/C.1.30

The Cartesian coordinates of $\underline{Q}_i$ are denoted by $(x_i, y_i, z_i)^T$. As noted in [3,4], coordinate axes may always be chosen such that

$$\sum_i x_i = 0, \quad \sum_i y_i = 0, \quad \sum_i x_i y_i = 0. \tag{2}$$

The two n dimensional vectors with ith entries x_i, y_i, are denoted by $\underline{x}$, $\underline{y}$, respectively, and the n dimensional vector with every entry equal to 1 is denoted by $\underline{e}$. The vectors $\hat{\underline{e}}$, $\hat{\underline{x}}$ and $\hat{\underline{y}}$ are defined as follows

$$\hat{\underline{e}} = \underline{e}/\|\underline{e}\|, \quad \hat{\underline{x}} = \underline{x}/\|\underline{x}\|, \quad \hat{\underline{y}} = \underline{y}/\|\underline{y}\|.$$

The n by 3 matrix with ith row equal to $(1, x_i, y_i)$ is denoted by E. Define d, σ by

$$d = \max\{\sqrt{x_i^2 + y_i^2} \mid 1 \leq i \leq n\} \tag{3}$$

$$\sigma = (\sqrt{n}d)\max\{1/\|\underline{x}\|, 1/\|\underline{y}\|\}, \tag{4}$$

under the assumption that co-ordinate axes have been chosen such that (2) holds. The quantity d measures the spread of the base points and σ measures the symmetry of their distribution. If the base points are colinear then σ is infinite. It is assumed that $d > 0$. The theoretical analysis given below is accurate provided d is small.

Let A be the n by 3 matrix with ith row equal to

$$(\underline{v}\cdot\underline{Q}_i)\underline{Q}_i^T - \underline{v}^T$$

and let $\underline{l}$ be the n dimensional vector with ith entry equal to

$$(\dot{\underline{Q}}_i \times \underline{Q}_i)\cdot\underline{v}.$$

The least-squares error function, $\varepsilon(\underline{v})$ [3,4], is defined on the unit sphere of hypothetical directions for the translational velocity as follows.

$$\varepsilon(\underline{v}) = \min\{\|A\underline{\Omega} - \underline{l}\| \mid \underline{\Omega} \in \mathbb{R}^3\}. \tag{5}$$

The function value, $\varepsilon(\underline{v})$, is the least-squares error associated with a best fit angular velocity, $\underline{\Omega}$, provided $\underline{v}$ is given. If $n < 4$ or $\hat{\underline{v}} = 0$ then $\varepsilon(\underline{v})$ is identically zero. From now on, it is assumed that $n \geq 4$, and as noted above, it is assumed that $\|\hat{\underline{v}}\| = 1$. The least-squares algorithm relies on a search for the local minima of $\varepsilon(\underline{v})$. Search strategies to locate these local minima will not be discussed; the error function itself is the main focus of interest.

The possibility of weighting the contributions of each flow vector to $\varepsilon(\underline{v})$ is not discussed. The aim is to obtain as complete an understanding of $\varepsilon(\underline{v})$ as possible, without the complications caused by such refinements. In practice, such a weighting may lead to more accurate results [5].

The following three properties of $\varepsilon(\underline{v})$ are obtained in [3,4]. Firstly, if $\varepsilon(\underline{v})$ is small then there exists an optical flow field, arising from a rigid body motion with translational velocity $\underline{v}$, which is very similar to the given optical flow field; secondly, the values of $\varepsilon(\underline{v})$ are independent of the angular velocity associated with the optical flow field; and thirdly, $\varepsilon(\underline{v})$ is approximated by $|a_3|\,\|\underline{t}\|$ where $\underline{t}$ is the n dimensional vector of errors in a linear least-squares approximation to the K_i. A more precise definition of $\underline{t}$ is given below.

The accuracy of the above approximation to $\varepsilon(\underline{v})$ is measured by the function

$$\Delta(\underline{v}) = |\varepsilon(\underline{v}) - |a_3|\,\|\underline{t}\||. \tag{6}$$

The main theoretical result of this paper is an upper bound on $\Delta(\underline{v})$. It is obtained by analysing the effect on $\varepsilon(\underline{v})$ of small perturbations in A.

The matrix A of (5) can be written in the form

$$A = EG^{-1} + C, \tag{7}$$

where

$$G^{-1} = \begin{bmatrix} -v_1 & -v_2 & 0 \\ v_3 & 0 & v_1 \\ 0 & v_3 & v_2 \end{bmatrix}$$

and C is defined by (7). It is assumed that $\det(G) \neq 0$, or equivalently,

$$v_3(v_1^2 + v_2^2) \neq 0.$$

(G^{-1} is defined in this way so that the inverse of a matrix does not appear in (8).) From the definitions of E and G^{-1}, it follows that EG^{-1} is the part of A linear in x_i, y_i. The equation

$$AG = E + CG \tag{8}$$

follows from (7). The n dimensional vectors $\underline{\alpha}$, $\underline{\beta}$, $\underline{\gamma}$ are used to denote the three columns of CG. It follows that

$$AG = [\underline{e} + \underline{\alpha} \mid \underline{x} + \underline{\beta} \mid \underline{y} + \underline{\gamma}]. \tag{9}$$

It is assumed throughout this paper that the three columns of AG are linearly independent. If (2) holds then these columns, $\underline{e} + \underline{\alpha}$, $\underline{x} + \underline{\beta}$, $\underline{y} + \underline{\gamma}$, are linearly independent provided

$$\|\lambda_1\hat{\underline{e}} + \lambda_2\hat{\underline{x}} + \lambda_3\hat{\underline{y}}\| > \|\lambda_1\underline{\alpha}/\sqrt{n} + \lambda_2\underline{\beta}/\|\underline{x}\| + \lambda_3\underline{\gamma}/\|\underline{y}\|\| \tag{10}$$

for all $\underline{\lambda} = (\lambda_1, \lambda_2, \lambda_3)^T$ with unit Euclidean norm. Inequality (10) certainly holds if

$$1 > \sqrt{3}\max\{\|\underline{\alpha}\|/\sqrt{n}, \|\underline{\beta}\|/\|\underline{x}\|, \|\underline{\gamma}\|/\|\underline{y}\|\}.$$

The bound on $\Delta(\underline{v})$ is obtained using the properties of the Moore-Penrose pseudo-inverse of a matrix [1]. The Moore-Penrose pseudo-inverse is a generalisation of the inverse of a matrix appropriate to finding a least-squares solution to an overdetermined set of linear equations. In detail, let $\underline{s}$ and $\underline{t}$ be the errors in the least-squares linear approximations to $\underline{l}$ and $\underline{K}$ respectively, where $\underline{K}$ is the n dimensional vector with ith entry equal to K_i. It follows from the definitions of $\underline{s}$ and $\underline{t}$ that

$$\|\underline{s}\| = \min\{\|E\underline{\Omega} - \underline{l}\| \mid \underline{\Omega} \in \mathbb{R}^3\}$$

$$\|\underline{t}\| = \min\{\|E\underline{\Omega} - \underline{K}\| \mid \underline{\Omega} \in \mathbb{R}^3\}.$$

It is shown in [1] that the vectors $\underline{s}$ and $\underline{t}$ are given by

$$\underline{s} = \underline{l} - EE^+\underline{l}, \quad \underline{y} = \underline{K} - EE^+\underline{K} \tag{11}$$

where

$$E^+ \equiv (E^TE)^{-1}E^T \tag{12}$$

is the Moore-Penrose pseudo-inverse of E. It is assumed that E^TE is invertible.

The Moore-Penrose pseudo-inverse has a simple geometrical interpretation [1]. The vector $EE^+\underline{l}$ is the normal projection of $\underline{l}$ onto the subspace of $\mathbb{R}^n$ spanned by the three columns of E. Similar remarks apply to $AA^+\underline{l}$. It follows from this geometrical interpretation that

$$\varepsilon(\underline{v}) = \|AA^{+}\underline{l} - \underline{l}\|. \tag{13}$$

It also follows from the geometrical interpretation of the Moore-Penrose pseudo-inverse that

$$(AA^{+})(AA^{+}) = AA^{+} \quad \text{and} \quad (AG)(AG)^{+} = AA^{+}. \tag{14}$$

The first equation of (14) follows from the fact that AA^{+} is a normal projection, and the second equation follows from the fact that the subspace of $\mathbb{R}^n$ spanned by the columns of A is identical to the subspace of $\mathbb{R}^n$ spanned by the columns of AG. The equations of (13) and (14) can also be proved algebraically using the fact that $A^{+} = (A^{T}A)^{-1}A^{T}$.

It is assumed from now on that coordinate axes have been chosen such that (2) holds. With this choice of axes, the three columns of E are orthogonal, and $E^{T}E$ is diagonal, namely

$$E^{T}E = \begin{bmatrix} n & 0 & 0 \\ 0 & \|\underline{x}\|^2 & 0 \\ 0 & 0 & \|\underline{y}\|^2 \end{bmatrix}. \tag{15}$$

The following expressions for $\underline{s}$ and $\underline{t}$ are obtained using the definition of E and (11), (12) and (15).

$$\underline{s} = \underline{l} - \overline{\underline{l}} - (\underline{l}\cdot\hat{\underline{x}})\hat{\underline{x}} - (\underline{l}\cdot\hat{\underline{y}})\hat{\underline{y}} \tag{16}$$

$$\underline{t} = \underline{K} - \overline{\underline{K}} - (\underline{K}\cdot\hat{\underline{x}})\hat{\underline{x}} - (\underline{K}\cdot\hat{\underline{y}})\hat{\underline{y}}, \tag{17}$$

where by definition, each component of $\overline{\underline{l}}$ is equal to $\overline{l}$, each component of $\overline{\underline{K}}$ is equal to $\overline{K}$, and $\overline{l}$, $\overline{K}$ are defined as follows.

$$\overline{l} = (1/n)\sum_i l_i, \qquad \overline{K} = (1/n)\sum_i K_i.$$

It follows from (16) and (17) that

$$\underline{s}\cdot\underline{e} = \underline{s}\cdot\underline{x} = \underline{s}\cdot\underline{y} = 0, \quad \underline{t}\cdot\underline{e} = \underline{t}\cdot\underline{x} = \underline{t}\cdot\underline{y} = 0. \tag{18}$$

The norms of E and E^{+} are easily calculated.

$$\|E\| = \sqrt{n}, \qquad \|E^{+}\| = \max\{1/\|\underline{x}\|,\ 1/\|\underline{y}\|\} \tag{19}$$

where the matrix norm $\|\cdot\|$ is subordinate to the Euclidean vector norm [1]. It follows that

$$\|E^{+}\| = \sigma/(\sqrt{n}d) \tag{20}$$

where σ is defined by (4).

II APPROXIMATING THE ERROR FUNCTION

An upper bound on $\Delta(\underline{v})$ is now obtained using the following strategy. An upper bound on $\Delta(\underline{v})$ involving four terms is found in Theorem 1, then upper bounds on each of these terms are found in Theorems 2, 3, 4 and 5, respectively. The four bounds are then brought together in Theorem 6. The reader may find it helpful to study the experimental results at the end of the paper before continuing with the theoretical analysis.

Theorem 1.

$$\Delta(\underline{v}) \leq \|(AA^{+} - EE^{+})\overline{\underline{l}}\| + \|(AA^{+} - EE^{+})[(\underline{l}\cdot\hat{\underline{x}})\hat{\underline{x}} + (\underline{l}\cdot\hat{\underline{y}})\hat{\underline{y}}]\| + \|(AA^{+} - EE^{+})\underline{s}\| + \|\underline{s} - a_3\underline{t}\| \tag{21}$$

where $\underline{l}$, $\overline{\underline{l}}$, $\underline{s}$ are obtained from the translational component of the optical flow field.

Proof. It may be supposed that $\underline{l}$, $\overline{\underline{l}}$, $\underline{s}$ are obtained from the translational component of the optical flow field, because both $\varepsilon(\underline{v})$ and $a_3\underline{t}$ are independent of the angular velocity. It follows from (6) and the triangle inequality [6] that

$$\Delta(\underline{v}) \leq \|AA^{+}\underline{l} - \underline{l} + a_3\underline{t}\|. \tag{22}$$

The first equation of (11) is used to substitute for the term $-\underline{l}$ of the right-hand side of (22), to yield

$$\Delta(\underline{v}) \leq \|AA^{+}\underline{l} - EE^{+}\underline{l} - \underline{s} + a_3\underline{t}\| \leq \|(AA^{+} - EE^{+})\underline{l}\| + \|\underline{s} - a_3\underline{t}\| \tag{23}$$

The result follows from (16), (23) and the triangle inequality [6].

Theorem 2.

$$\|(AA^{+} - EE^{+})\overline{\underline{l}}\| \leq (|a_3|\overline{K} + |\overline{m}|)\|\underline{\alpha}'\| \tag{24}$$

where $\underline{\alpha}'$ is the component of $\underline{\alpha}$ normal to $\underline{e} + \underline{\alpha}'$ and $\overline{m}$ is the mean value of the components of the vector

$$m_i = (\underline{v}\times\hat{\underline{v}})\cdot(\underline{Q}_i - \underline{Q})(K_i - \overline{K}) + (\underline{v}\times\hat{\underline{v}})_3(z_i - 1)\overline{K}, \tag{25}$$

Proof. It follows from (2), (14) and the definition of E that

$$\|(AA^{+} - EE^{+})\overline{\underline{l}}\| = \|(AG)(AG)^{+}\overline{\underline{l}} - \overline{\underline{l}}\|. \tag{26}$$

The right-hand side of (26) is equal to the minimum distance from $\overline{\underline{l}}$ to the subspace of $\mathbb{R}^n$ spanned by the columns of AG. This distance is less than or equal to the minimum distance from $\overline{\underline{l}}$ to the subspace of $\mathbb{R}^n$ spanned by $\underline{e} + \underline{\alpha}$. Now $\overline{\underline{l}} + \overline{l}\underline{\alpha}$ is in the subspace of $\mathbb{R}^n$ spanned by $\underline{e} + \underline{\alpha}$, thus

$$\|(AG)^{+}\overline{\underline{l}}\| \leq |\overline{l}|\,\|\underline{\alpha}'\|. \tag{27}$$

An upper bound for $|\overline{l}|$ is now obtained. It follows from (25) that the vector $\underline{l}$ can be expanded in the form

$$\underline{l} = [(\underline{v}\times\hat{\underline{v}})\cdot\underline{Q}]\underline{K} + [(\underline{v}\times\hat{\underline{v}})_1\underline{x} + (\underline{v}\times\hat{\underline{v}})_2\underline{y}]\overline{K} + \underline{m}. \tag{28}$$

The equations of (2) and (28) together yield

$$\overline{\underline{l}} = a_3\overline{\underline{K}} + \overline{\underline{m}}$$

thus

$$|\overline{l}| \leq |a_3|\overline{K} + |\overline{m}|. \tag{29}$$

Inequality (24) now follows from (27) and (29).

Theorem 3.

$$\|(AA^{+} - EE^{+})[(\underline{l}\cdot\hat{\underline{x}})\underline{x} + (\underline{l}\cdot\hat{\underline{y}})\hat{\underline{y}}]\| \leq [\sigma/(nd)]\Lambda\sqrt{(\underline{l}\cdot\hat{\underline{x}})^2 + (\underline{l}\cdot\hat{\underline{y}})^2}$$

where

$$\Lambda = \sqrt{n}\sqrt{\|\underline{\beta}_{\perp}\|^2 + \|\underline{\gamma}_{\perp}\|^2} + \|\underline{\alpha}\|\sqrt{\|\underline{\beta}_{\parallel}\|^2 + \|\underline{\gamma}_{\parallel}\|^2},$$

and

$$\underline{\beta}_{\perp} = \underline{\beta} - (\underline{\beta}\cdot\hat{\underline{e}})\hat{\underline{e}}, \qquad \underline{\beta}_{\parallel} = (\underline{\beta}\cdot\hat{\underline{e}})\hat{\underline{e}}$$

$$\underline{\gamma}_{\perp} = \underline{\gamma} - (\underline{\gamma}\cdot\hat{\underline{e}})\hat{\underline{e}}, \qquad \underline{\gamma}_{\parallel} = (\underline{\gamma}\cdot\hat{\underline{e}})\hat{\underline{e}}.$$

Proof. It follows from (2), (14) and the definition of E that

$$\|(AA^+ - EE^+)[(\underline{l}\cdot\hat{\underline{x}})\hat{\underline{x}} + (\underline{l}\cdot\hat{\underline{y}})\hat{\underline{y}}]\| =$$

$$\|(AG)(AG)^+[(\underline{l}\cdot\hat{\underline{x}})\hat{\underline{x}} + (\underline{l}\cdot\hat{\underline{y}})\hat{\underline{y}}] - [(\underline{l}\cdot\hat{\underline{x}})\hat{\underline{x}} + (\underline{l}\cdot\hat{\underline{y}})\hat{\underline{y}}]\| \tag{30}$$

The right-hand side of (30) is equal to the minimum distance from $[(\underline{l}\cdot\hat{\underline{x}})\hat{\underline{x}} + (\underline{l}\cdot\hat{\underline{y}})\hat{\underline{y}}]$ to the subspace of $\mathbb{R}^n$ spanned by the columns of AG. An upper bound is found for the right-hand side of (30) by constructing a vector in this subspace close to $[(\underline{l}\cdot\hat{\underline{x}})\hat{\underline{x}} + (\underline{l}\cdot\hat{\underline{y}})\hat{\underline{y}}]$. This vector is

$$(\underline{l}\cdot\hat{\underline{x}})\hat{\underline{x}} + (\underline{l}\cdot\hat{\underline{y}})\hat{\underline{y}} + (\underline{l}\cdot\hat{\underline{x}})\underline{\beta}_\perp/\|\underline{x}\| +$$

$$(\underline{l}\cdot\hat{\underline{y}})\underline{\gamma}_\perp/\|\underline{y}\| - \underline{\chi}, \tag{31}$$

where

$$\underline{\chi} = [(\underline{l}\cdot\hat{\underline{x}})(\underline{\beta}\cdot\hat{\underline{e}})/\|\underline{x}\| + (\underline{l}\cdot\hat{\underline{y}})(\underline{\gamma}\cdot\hat{\underline{e}})/\|\underline{y}\|]\underline{\alpha}/\sqrt{n}. \tag{32}$$

The vector of (31) is in the subspace of $\mathbb{R}^n$ spanned by the columns of AG since it can be written in the form

$$[(\underline{l}\cdot\hat{\underline{x}})/\|\underline{x}\|][\underline{x} + \underline{\beta} - (\underline{\beta}\cdot\hat{\underline{e}})(\underline{e} + \underline{\alpha})/\sqrt{n}] +$$

$$[(\underline{l}\cdot\hat{\underline{y}})/\|\underline{y}\|][\underline{y} + \underline{\gamma} - (\underline{\gamma}\cdot\hat{\underline{e}})(\underline{e} + \underline{\alpha})/\sqrt{n}].$$

It follows from (30) and the construction of (31) that

$$\|(AA^+ - EE^+)[(\underline{l}\cdot\hat{\underline{x}})\hat{\underline{x}} + (\underline{l}\cdot\hat{\underline{y}})\hat{\underline{y}}]\| \leq \|\underline{b}\|. \tag{33}$$

where

$$\underline{b} = (\underline{l}\cdot\hat{\underline{x}})\underline{\beta}_\perp/\|\underline{x}\| + (\underline{l}\cdot\hat{\underline{y}})\underline{\gamma}_\perp/\|\underline{y}\| - \underline{\chi}. \tag{34}$$

An upper bound is now obtained for $\|\underline{b}\|$. It follows from (4), (34) and the triangle inequality [6] that

$$\|\underline{b}\| \leq [\sigma/(\sqrt{n}d)][|\hat{\underline{x}}\cdot\underline{l}|\ \|\underline{\beta}_\perp\| + |\hat{\underline{y}}\cdot\underline{l}|\ \|\underline{\gamma}_\perp\|] + \|\underline{\chi}\|. \tag{35}$$

On applying the Cauchy-Schwartz inequality [6] to (35), the inequality

$$\|\underline{b}\| \leq$$

$$[\sigma/(\sqrt{n}d)]\sqrt{(\underline{l}\cdot\hat{\underline{x}})^2 + (\underline{l}\cdot\hat{\underline{y}})^2}\ \sqrt{\|\underline{\beta}_\perp\|^2 + \|\underline{\gamma}_\perp\|^2} + \|\underline{\chi}\|. \tag{36}$$

is obtained. The Cauchy-Schwartz inequality is also applied to (32) to obtain

$$\|\underline{\chi}\| \leq [\sigma\|\underline{\alpha}\|/(nd)]\sqrt{(\underline{l}\cdot\hat{\underline{x}})^2 + (\underline{l}\cdot\hat{\underline{y}})^2}\ \sqrt{\|\underline{\beta}_\parallel\|^2 + \|\underline{\gamma}_\parallel\|^2}. \tag{37}$$

The result follows from (33), (36) and (37).

Theorem 4.

$$\|(AA^+ - EE^+)\underline{s}\| \leq$$

$$[\sigma/(\sqrt{n}d)]\sqrt{(\underline{s}\cdot\underline{\beta})^2 + (\underline{s}\cdot\underline{\gamma})^2}\ [1+0(d)].$$

Proof. It follows from (2), (14), (18) and the definition of E that

$$\|(AA^+ - EE^+)\underline{s}\| = \|(AG)(AG)^+\underline{s}\|.$$

The vector $(AG)(AG)^+\underline{s}$ is the projection of $\underline{s}$ onto the subspace of $\mathbb{R}^n$ spanned by the columns of AG. It follows that

$$\|(AG)(AG)^+\underline{s}\| \leq$$

$$\max\{|\underline{s}\cdot\underline{w}|\ \ |\ \ \underline{w} \neq 0 \text{ and } \underline{w}/\|\underline{w}\| \in B_2\} \tag{38}$$

where B_2 is the two-dimensional sphere of vectors in $\mathbb{R}^n$ that are of unit Euclidean norm and that are also linear combinations of the columns of AG.

In order to prove the theorem, an alternative description of B_2 is obtained, as the range of a continuous function, $\underline{f}(\underline{\lambda})$, from the unit sphere to B_2. The function $\underline{f}(\underline{\lambda})$ is defined by $\underline{f}(\underline{\lambda}) = \underline{w}(\underline{\lambda})/\|\underline{w}(\underline{\lambda})\|$ where $\underline{\lambda}$ is any three-dimensional vector of unit Euclidean norm, and $\underline{w}(\underline{\lambda})$ is given by

$$\underline{w}(\underline{\lambda}) = \lambda_1(\hat{\underline{e}} + \underline{\alpha}/\sqrt{n}) + \lambda_2(\hat{\underline{x}} + \underline{\beta}/\|\underline{x}\|) +$$

$$\lambda_3(\hat{\underline{y}} + \underline{\gamma}/\|\underline{y}\|). \tag{39}$$

The function $\underline{f}(\underline{\lambda})$ is well defined provided $\underline{w}(\underline{\lambda}) \neq 0$, but this is always the case, since the vectors $\hat{\underline{e}} + \underline{\alpha}/\sqrt{n}$, $\hat{\underline{x}} + \underline{\beta}/\|\underline{x}\|$ and $\hat{\underline{y}} + \underline{\gamma}/\|\underline{y}\|$ are assumed to be linearly independent. The linear independent of these three vectors is also sufficient to ensure that $\underline{f}(\underline{\lambda})$ maps onto B_2, since any vector in B_2 can be expressed as a linear combination of $\hat{\underline{e}} + \underline{\alpha}/\sqrt{n}$, $\hat{\underline{x}} + \underline{\beta}/\|\underline{x}\|$ and $\hat{\underline{y}} + \underline{\gamma}/\|\underline{y}\|$.

As $\underline{f}(\underline{\lambda})$ maps onto B_2, it follows that

$$\|(AG)(AG)^+\underline{s}\| \leq \max\{|\underline{s}\cdot\underline{f}(\underline{\lambda})|\ \ |\ \ \|\underline{\lambda}\| = 1\}$$

$$\leq \max\{|\underline{s}\cdot\underline{w}(\underline{\lambda})|/\|\underline{w}(\underline{\lambda})\|\ \ |\ \ \|\underline{\lambda}\| = 1\}. \tag{40}$$

Equations (18) and (39) together yield

$$\underline{s}\cdot\underline{w}(\underline{\lambda}) = \lambda_1(\underline{s}\cdot\underline{\alpha})/\sqrt{n} + \lambda_2(\underline{s}\cdot\underline{\beta})/\|\underline{x}\| + \lambda_3(\underline{s}\cdot\underline{\gamma})/\|\underline{y}\|$$

$$= \lambda_2(\underline{s}\cdot\underline{\beta})/\|\underline{x}\| + \lambda_3(\underline{s}\cdot\underline{\gamma})/\|\underline{y}\| + 0(d^2\|\underline{s}\|)$$

thus

$$\underline{s}\cdot\underline{w}(\underline{\lambda})/\|\underline{w}(\underline{\lambda})\|$$

$$\leq [\sigma/(\sqrt{n}d)]\|\lambda_2(\underline{s}\cdot\underline{\beta}) + \lambda_3(\underline{s}\cdot\underline{\gamma})\|[1 + 0(d)]/\|\underline{w}(\underline{\lambda})\|. \tag{41}$$

The result now follows from (40), (41), the fact that $\underline{\lambda}$ has unit Euclidean norm and the fact that

$$\|\underline{w}(\underline{\lambda})\| = 1 + 0(d).$$

Theorem 5.

$$\|\underline{s} - a_3\underline{t}\| = \|\underline{m} - EE^+\underline{m}\|,$$

provided $\underline{s}$ is obtained from the translational component of the optical flow field.

Proof. The matrix $I - EE^+$ (where I is the n by n identity matrix) is applied to (28) to obtain

$$\underline{l} - EE^+\underline{l} = a_3(\underline{K} - EE^+\underline{K}) + \underline{m} - EE^+\underline{m}. \tag{42}$$

The result follows from (11) and (42).

Theorem 6.

$$\Delta(\underline{v}) \leq B(\underline{v})$$

where $B(\underline{v})$ is defined by

$$B(\underline{v}) = (|a_3|\overline{K} + |\overline{m}|\ \|\underline{\alpha}'\| +$$

$$[\sigma/(nd)]\Lambda\sqrt{(\underline{l}\cdot\hat{\underline{x}})^2 + (\underline{l}\cdot\hat{\underline{y}})^2} +$$

$$[\sigma/(\sqrt{n}d)]\ \sqrt{(\underline{s}\cdot\underline{\beta})^2 + (\underline{s}\cdot\underline{\gamma})^2}[1 + 0(d)] +$$

$$\|\underline{m} - EE^+\underline{m}\|. \tag{43}$$

and $\underline{l}$, $\underline{s}$, $\underline{m}$ are obtained from the translational component of the optical flow field.

Proof. The result follows from Theorems 1, 2, 3, 4 and 5.

Theorem 6 is a more accurate version of the result in [3] that $\Delta(\underline{v}) = 0(d^2)$. It can be demonstrated that Theorem 6 yields $\Delta(\underline{v})\ 0(d^2)$ by obtaining estimates of the various terms on the right-hand side of (43). It follows from (8) and (9) that

$$\|\underline{\alpha}\| = O(d^2), \quad \|\underline{\beta}\| = O(d^2), \quad \|\underline{\gamma}\| = O(d^2) \qquad (44)$$

thus

$$|\underline{s}\cdot\underline{\beta}| = O(d^2\|\underline{s}\|), \qquad |\underline{s}\cdot\underline{\gamma}| = O(d^2\|\underline{s}\|). \qquad (45)$$

In most cases of practical interest, $|K_i - \bar{K}| = O(d\|\underline{K}\|)$ and $\bar{K} = O(\|\underline{K}\|/\sqrt{n})$. It follows that

$$|\underline{l}\cdot\hat{\underline{x}}| = O(d\|\underline{K}\|), \quad |\underline{l}\cdot\hat{\underline{y}}| = O(d\|\underline{K}\|)$$

$$|\bar{m}| = O(d^2\|\underline{K}\|). \qquad (46)$$

The estimates of (44) yield

$$\Lambda = O(d^2) \qquad (47)$$

where Λ is as defined in Theorem 3. The result $\Delta(\underline{v}) \leq B(\underline{v}) = O(d^2\|\underline{K}\|)$ now follows from Theorem 6, (43), (44), (45), (46) and (47).

A major drawback to (43) is that the terms on the right-hand side of (43) are not expressed in terms of immediate physical interest, such as $\hat{\underline{v}}$, $\underline{v}$, $\underline{x}$, $\underline{y}$ and $\underline{K}$. An upper bound for $\Delta(\underline{v})$ depending on these terms is obtained in [4], but with a considerable loss of accuracy.

As explained in [3,4], it follows from the approximation

$$\varepsilon(\underline{v}) \approx |a_3|\,\|\underline{t}\| = |v_1\hat{v}_2 - v_2\hat{v}_1|\,\|\underline{t}\|$$

that accurate estimates of $\tan^{-1}(\hat{v}_1/\hat{v}_2)$ can be recovered from optical flow fields arising from irregular moving surfaces, provided $\hat{\underline{v}}$ is not close to $(0, 0, 1)^T$. It is also shown in [3] that the component of $\hat{\underline{\Omega}}$ in the direction $(\hat{v}_1, \hat{v}_2, 0)^T$, namely,

$$(\hat{v}_1\hat{\Omega}_1 + \hat{v}_2\hat{\Omega}_2)/\sqrt{\hat{v}_1^2 + \hat{v}_2^2}$$

can be expressed in terms of $\hat{v}_1/\hat{v}_2$ and the zero order terms of the optical flow field.

It is now shown that σ is bounded below by $\sqrt{2}$. It follows from (3) that

$$\|\underline{x}\|^2 + \|\underline{y}\|^2 \leq nd^2,$$

thus

$$\min\{\|\underline{x}\|^2, \ \|\underline{y}\|^2\} \leq nd^2/2,$$

thus

$$\max\{1/\|\underline{x}\|, \ 1/\|\underline{y}\|\} \geq \sqrt{2}/(\sqrt{n}d).$$

The result that $\sigma \geq \sqrt{2}$ now follows.

A heuristic argument is now given to show that $\sigma \approx 2$, provided there are a large number of base points scattered uniformly throughout a disk of radius d, centred at $(0, 0, 1)^T$. The number of base points in a small area $\Delta x\Delta y$ is approximately equal to $n\Delta x\Delta y/(\pi d^2)$, thus

$$\|\underline{x}\|^2 = \sum_i x_i^2 \approx n\sum_i x_i^2\Delta x\Delta y/(\pi d^2) \qquad (48)$$

where the right-most summation of (48) is over small areas of the form $\Delta x\Delta y$. It follows that

$$\|\underline{x}\|^2 \approx n\iint x^2 dx\,dy/(\pi d^2) = nd^2/4.$$

A similar argument yields $\|\underline{y}\|^2 \approx nd^2/4$. The result $\sigma \approx 2$ now follows.

III EXPERIMENTAL RESULTS

The accuracy of the bound $B(\underline{v})$ on $\Delta(\underline{v})$ given in Theorem 6 has been assessed using computer-generated data. A typical set of experimental results is shown in Figure 1 at the end of this paper. The four graphs in Figure 1 are obtained by plotting the values of

$$\varepsilon(\underline{v}), \ |a_3|\,\|\underline{t}\|, \ \varepsilon(\underline{v}) + B(\underline{v}) \text{ and } \varepsilon(\underline{v}) - B(\underline{v})$$

as ϕ varies, where the unit vector $\underline{v}$ is given by

$$\underline{v} = (\sqrt{2}\cos(\phi)/\sqrt{3}, \ \sqrt{2}\sin(\phi)/\sqrt{3}, \ 1/\sqrt{3})^T.$$

The values of ϕ are shown by the axis labelled 'ϕ deg'. The true value $\hat{\underline{v}}$ of the translational velocity is marked on the ϕ axis with a '^'.

The four curves in Figure 1 are represented by

* $\varepsilon(\underline{v})$

\+ $|a_3|\,\|\underline{t}\|$

. $\begin{cases} \varepsilon(\underline{v}) + B(\underline{v}) \\ \varepsilon(\underline{v}) - B(\underline{v}) \end{cases}$

The '+'s marking points on the curve defined by $|a_3|\,\|\underline{t}\|$ are frequently overwritten by the '*'s marking points on the curve defined by $\varepsilon(\underline{v})$.

The computer-generated optical flow field used to obtain Figure 1 arises from a rigid moving surface consisting of two planar facets with outward normals $(\cos(\zeta), 0, -\sin(\zeta))^T$ and $(-\cos(\zeta), 0, -\sin(\zeta))^T$ respectively. The surface forms a 'peak' pointing towards the projection sphere. The true translational velocity $\hat{\underline{v}}$ is set to equal $(1/\sqrt{3}, 1/\sqrt{3}, 1/\sqrt{3})^T$ and the angular velocity is set to zero. The flow vectors are scaled to have average length d/5, and d is set equal to 0.1 radians. (The figure d/5 is suggested by typical optical flow fields arising in practice.) The following five base points are used

$(0, 0, 1)^T$, $(d, 0, \sqrt{1 - d^2})^T$,

$(0, d, \sqrt{1 - d^2})^T$, $(-d, 0, \sqrt{1 - d^2})^T$,

$(0, -d, \sqrt{1 - d^2})^T$.

It is clear from Figure 1 that $|a_3|\,\|\underline{t}\|$ is a very accurate approximation to $\varepsilon(\underline{v})$, that is,

$$|\varepsilon(\underline{v}) - |a_3|\,\|\underline{t}\|\,| \quad \ll \quad |a_3|\,\|\underline{t}\|,$$

provided the rigid body surface is irregular. Figure 1 also shows that the theory given above yields only a partial explanation of this accuracy, since $B(\underline{v})$ is many times larger than $\Delta(\underline{v})$.

A more extensive experimental investigation, described in [4], shows that $\Delta(\underline{v})$ remains small even for values of d as high as 0.5 radians; unfortunately, $B(\underline{v})$ is much greater than $\Delta(\underline{v})$ for such values of d. The investigation also shows that $\Delta(\underline{v})$ becomes greater as the peak in the moving rigid surface becomes less prominent, that is, as ζ becomes large. If ζ is greater than about 1.0 radians then $\varepsilon(\underline{v})$ is no longer well approximated by $|a_3|\,\|\underline{t}\|$.

The effects of noise on $\varepsilon(\underline{v})$ are investigated in [4]. Experimental results show that a 4% perturbation in the optical flow field described above causes an error of about 0.14 radians in the estimate of $\tan^{-1}(\hat{v}_1/\hat{v}_2)$. A theoretical argument is given in [4] to show that the effects of noise decrease as 1/d becomes small.

IV A WEAK POINT IN THE THEORY

It is clear from the experimental results given above that $\Delta(\underline{v}) \ll B(\underline{v})$. A short experimental investigation was carried out to discover the step in the above theoretical analysis at which the upper bounds obtained for $\Delta(\underline{v})$ begin to differ widely from $\Delta(\underline{v})$. The biggest contribution to this difference was found in the step

$$|\varepsilon(\underline{v}) - |a_3| \, \|\underline{t}\| \, | \leq \|AA^{+}\underline{l} - \underline{l} + a_3\underline{t}\|$$

made in the proof of Theorem 1. Experimental results obtained using the rigid surface and base points specified above show that most of the discrepancy between $\Delta(\underline{v})$ and $B(\underline{v})$ arises from the difference in direction of the two vectors $AA^{+}\underline{l} - \underline{l}$ and $a_3\underline{t}$. If $d = 0.1$ radians, then this difference in direction is also about 0.1 radians. The lengths of the two vectors are very similar.

The methods used in this paper are sufficient to prove that the difference between $\|AA^{+}\underline{l} - \underline{l}\|$ and $|a_3| \, \|\underline{t}\|$ is $O(d)$, however, it is conjectured that this difference is, in fact, $O(d^2)$, provided the optical flow field arises from an irregular rigid moving surface.

ACKNOWLEDGEMENTS

The material in this paper forms part of a thesis on optical flow [4] based on work carried out as part of RSRE contract MW41B/940. The author acknowledges the support of ESPRIT Project P940 during the writing of this paper. The author thanks the Marconi Company for its support and he thanks the Technical Director of the Marconi Company for permission to publish. The author also thanks George Loizou for his constant advice and encouragement.

REFERENCES

1 Golub, G. H. and C. F. Van Loan. Matrix Computations. North Oxford (1983).

2 Longuet-Higgins, H. C. and K. Prazdny. "The interpretation of a moving retinal image" Proc. Roy. Soc. Lond. Series B Vol 208 (1980) pp 385-397.

3 Maybank, S. J. "Algorithm for analysing optical flow based on the least squares method" Image Vision Comput. Vol 4 (1986) pp 38-42.

4 Maybank, S. J. A theoretical study of optical flow. Ph.D. thesis, Birkbeck College, University of London, U.K. (1987) (in preparation).

5 Scott, G. Local and global interpretation of images. Ph.D. thesis, University of Sussex, U.K. (1986).

6 Sokolnikoff, I. S. and R. M. Redheffer. Mathematics of Physics and Modern Engineering. McGraw-Hill. (1966).

7 Yen, B. L. and T. S. Huang. "Determining 3-D motion and structure of a rigid body using the spherical projection". Comput. Vision Graph. Image Process. Vol 21 (1983) pp 21-32.

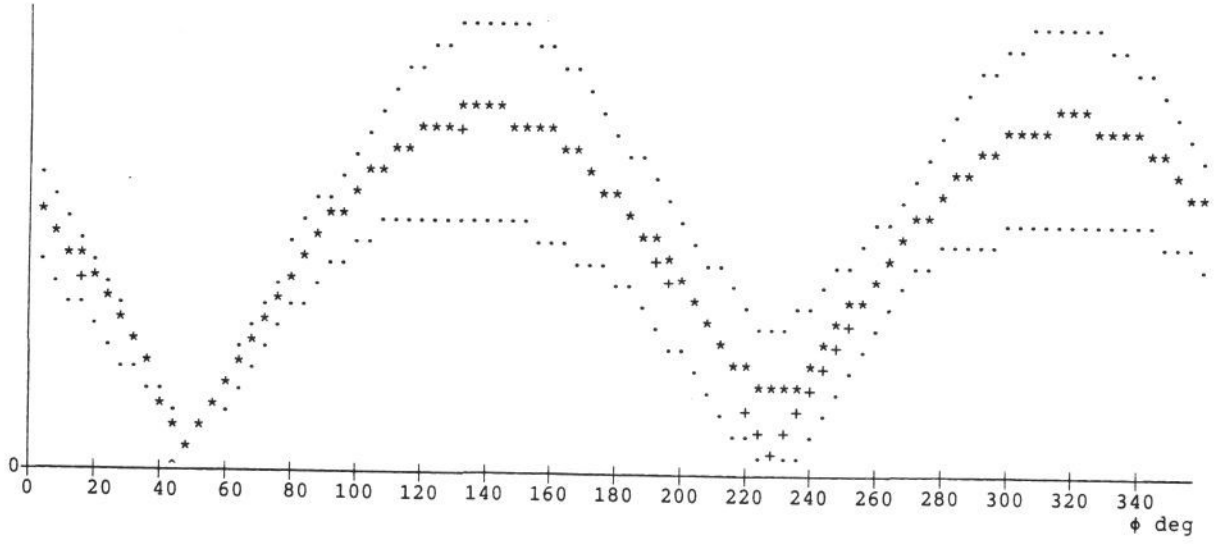

Figure 1. Graph of $\varepsilon(\underline{v})$ evaluated on the circle $v_3 = 1/\sqrt{3}$